

Southern Ocean buoyancy forcing of ocean ventilation and glacial atmospheric CO₂

Andrew J. Watson^{1*}, Geoffrey K. Vallis² and Maxim Nikurashin^{3,4}

Atmospheric CO₂ concentrations over glacial-interglacial cycles closely correspond to Antarctic temperature patterns¹. These are distinct from temperature variations in the mid to northern latitudes², so this suggests that the Southern Ocean is pivotal in controlling natural CO₂ concentrations³. Here we assess the sensitivity of atmospheric CO₂ concentrations to glacial-interglacial changes in the ocean's meridional overturning circulation using a circulation model^{4,5} for upwelling and eddy transport in the Southern Ocean coupled with a simple biogeochemical description. Under glacial conditions, a broader region of surface buoyancy loss results in upwelling farther to the north, relative to interglacials. The northern location of upwelling results in reduced CO₂ outgassing and stronger carbon sequestration in the deep ocean: we calculate that the shift to this glacial-style circulation can draw down 30 to 60 ppm of atmospheric CO₂. We therefore suggest that the direct effect of temperatures on Southern Ocean buoyancy forcing, and hence the residual overturning circulation, explains much of the strong correlation between Antarctic temperature variations and atmospheric CO₂ concentrations over glacial-interglacial cycles.

The Southern Ocean is where the dense water that makes up most of the ocean interior upwells to the surface, and is also the site of formation of Antarctic Bottom Water (AABW), and Antarctic Intermediate Water⁶ (AAIW). These, together with North Atlantic Deep Water (NADW) form the intermediate and deep waters of the world ocean. The deep ocean is the main repository for inorganic carbon (predominantly as bicarbonate and carbonate ions) in the ocean–atmosphere system, so processes affecting its ventilation can influence atmospheric CO₂. The Southern Ocean meridional overturning circulation (MOC) responds to surface forcing from the atmosphere, both from the circumpolar westerly winds, and through changes in surface buoyancy due to heat fluxes, precipitation and ice formation or melt⁶. There have been a number of studies of the impact on CO₂, via the MOC, of changes in the westerly wind belt^{7–9}, and of sea ice-related effects^{10,11}, but the effect of alterations in buoyancy forcing, although noted^{12,13}, has not previously been quantitatively studied.

Figure 1 shows a schematic of the present-day and Last Glacial Maximum (LGM) ocean overturning circulations. Deep water upwells in the Southern Ocean, under the influence of the westerly winds that cause an Ekman drift of surface waters to the north. This drift causes the isopycnals to steepen, and the Antarctic Circumpolar Current is in part the geostrophic response to this forcing. Baroclinic instability in the current generates eddies that mediate a net flux to the south near the surface, tending to flatten the

isopycnals. At steady state, the net residual overturning is the difference between northward wind-driven and southward eddy fluxes, and is constrained by the requirement that the buoyancy budget is balanced⁶. If upwelling water reaching the surface becomes lighter because heat or fresh water is added to it from the atmosphere then this balance will be satisfied by an increased net northward flow. Conversely, if upwelling water loses buoyancy on reaching the surface, by cooling and/or sea ice formation and brine rejection, then we expect enhanced near-surface flow southwards⁶. Wind forcing is therefore not the only factor determining how tracers are advected by the MOC: the buoyancy budget strongly influences how much upwelling occurs, and whether upwelled water joins the upper or the lower overturning cell¹³.

Atmospheric carbon dioxide is heavily influenced by the biological activity in surface waters, and most particularly by the amount of carbon that has been removed by plankton from waters feeding the deep source regions. Under rather general assumptions (see Methods), the drawdown in atmospheric CO₂ has been shown to be related to the 'preformed' nutrient content of deep water¹⁴, this being the amount of phosphate limiting nutrient that remains unused by the biota when the water leaves the surface layer. In deep water formed in the modern Southern Ocean, preformed phosphate is high¹⁴, because the biota are unable to utilize all of the nutrient during the relatively short residence time of the water at the surface between upwelling and subduction to form either AABW or AAIW. Whereas under favourable bloom conditions the biota can consume surface nutrients in a matter of weeks, the timescale for biological utilization of nutrient in the polar Southern Ocean is of the order of a year or longer, owing to the deep mixed layer, lack of light through the winter, and the limited supply of iron. The resulting productivity is sufficient to deplete only a modest fraction of the available nutrient. Processes that slow ocean ventilation so that water spends longer in the surface layer, that increase the separation between upwelling and downwelling regions, or speed up the biological response time will result in more efficient nutrient and carbon uptake. Maintained for times of centuries sufficient to affect the deep ocean carbon content, this would lower atmospheric CO₂ concentrations.

In glacial time we would expect a substantial contraction of the zone of net buoyancy gain and expansion of the region of buoyancy loss over the Southern Ocean, due to the colder atmosphere and weaker hydrologic cycle. With the deep water upwelling to the surface already near the freezing point¹⁵, and much more extensive ice cover, overall buoyancy loss fluxes might be weak. At present, much of the water upwelling to the surface in the polar ice-free zone moves north on reaching the surface to join the upper cell, as a

¹College of Life and Environmental Sciences, University of Exeter, Laver Building, North Park Road, Exeter EX4 4QE, UK. ²College of Engineering, Mathematics and Physics, University of Exeter, Harrison Building, North Park Road, Exeter EX4 4QF, UK. ³Institute for Marine and Antarctic Studies, University of Tasmania, Private Bag 129, Hobart, Tasmania 7001, Australia. ⁴ARC Centre of Excellence for Climate System Science, Sydney, New South Wales, Australia. *e-mail: andrew.watson@exeter.ac.uk

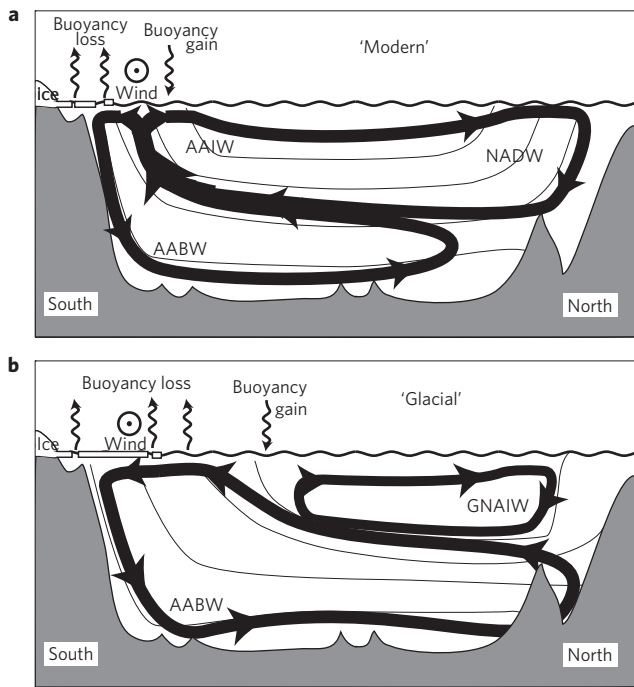


Figure 1 | Schematic of the global overturning with emphasis on the Southern Ocean, in the present day and at LGM. Thin lines represent density surfaces. **a**, Modern ocean: NADW and AABW upwell in the Southern Ocean under the influence of the wind. At the surface, southward eddy fluxes dominate where there is surface buoyancy loss, and northward Ekman flux dominates where there is buoyancy gain. **b**, LGM: a broader region of buoyancy loss gives upwelling at further distance from the Antarctic continent, farther from the region of AABW formation. Glacial North Atlantic Intermediate Water (GNAIW) is sufficiently light that there is no isopycnal pathway allowing it to return to the surface in the Southern Ocean.

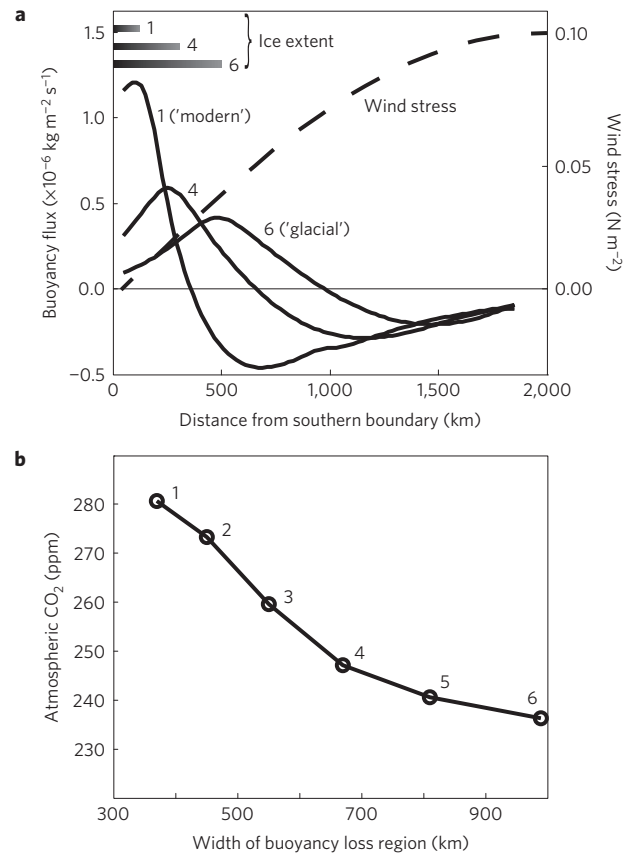


Figure 2 | Forcings and results from the numerical model described in the text and Methods. **a**, Buoyancy fluxes, ice coverage and wind stress across the southern channel. Solid lines show 'modern', 'glacial' and an intermediate distribution of buoyancy flux (positive values are buoyancy loss). Ice extent is shown at the top, with fractional coverage shown as depth of shading. Numbers refer to the points in **b**. The same wind stress (dashed line) is used throughout. **b**, Steady-state atmospheric CO₂ for buoyancy forcings going from (1) modern to (6) glacial. Changes in CO₂ are those due solely to overturning circulation changes; in practice the implied lower surface temperatures would further enhance the CO₂ reduction in the glacial simulations.

both buoyancy and CO₂ exchange with the atmosphere. Figure 2a shows the buoyancy fluxes and area affected by ice. The buoyancy loss region (positive values in Fig. 2a) is concentrated towards the southern boundary in the 'modern' case, and extends progressively farther north as one moves to the 'glacial' simulation. In Fig. 2b, CO₂ concentration is plotted against the width of the region of net buoyancy loss—it decreases by ~45 ppm from modern to glacial simulations. Figure 3 shows the overturning circulation in the modern and glacial cases, together with more detailed views of the near-surface southern channel. With the modern forcing, the intense and southerly located upwelling results in water feeding the lower cell having only a short residence time at the surface. Phosphate concentrations remain high when they reach the southern boundary, where most of the deep water sinking of the lower overturning cell occurs. The glacial circulation is less intense and upwells farther to the north, more distant from the region where water joining the lower cell leaves the surface. This allows a longer residence time for the water at the surface, and more time for the biota to draw down nutrients and CO₂, so that the source water for the lower cell has less preformed nutrient. There is good evidence that biological productivity can continue in and under sea ice, depending on its thickness²². However, the blocking by ice of air–sea CO₂ exchange acts to reduce the CO₂ drawdown in the more strongly glacial simulations.

Q.6

1 result of the net input of heat and fresh water from the atmosphere.
2 This cell is vigorous, variously estimated at 10–20 Sv today^{16,17},
3 the range reflecting both genuine uncertainty and different ways
4 of defining the flow. Much of this upwelling ultimately balances
5 the sinking in the North Atlantic—given that diapycnal mixing
6 in mid-waters of the ocean basins is weak¹⁸, most of the NADW
7 formation is 'pulled' by Southern Ocean upwelling via isopycnal
8 transport¹⁹. The implication is that a vigorous upper cell can be
9 supported only if the density set by convection in northern latitudes
10 allows an isopycnal pathway that can upwell in the Southern Ocean,
11 and that the strength of this overturning is greatly influenced
12 by buoyancy forcing in the south that allows this closure of the
13 circulation²⁰. Under glacial conditions, most palaeoceanographic
14 proxies²¹ suggest that this circulation was weakened, with Glacial
15 North Atlantic Intermediate Water, which replaced NADW in the
16 Atlantic, not extending as far into the Southern Ocean, implying
17 less overlap between northern and southern component densities.
18 This would be in accord with a regime in the south in which a
19 broader region of buoyancy loss directed surface flow there towards
20 the lower cell at LGM, as shown in Fig. 1b.

Q.7

21 Figure 2 shows some results obtained from a two-dimensional
22 numerical model⁵ of the overturning circulation, with the addition
23 of a minimal biogeochemical scheme, to changing buoyancy
24 forcings across the circumpolar channel that represents the Southern
25 Ocean (see Methods). In the integrations shown, wind stress
26 across this channel was unchanged between runs, as was buoyancy
27 forcing in the northern basin. We imposed Southern Ocean buoyancy
28 fluxes, and included the effect of ice formation at the surface
29 as the water cools towards freezing, with the ice covering impeding

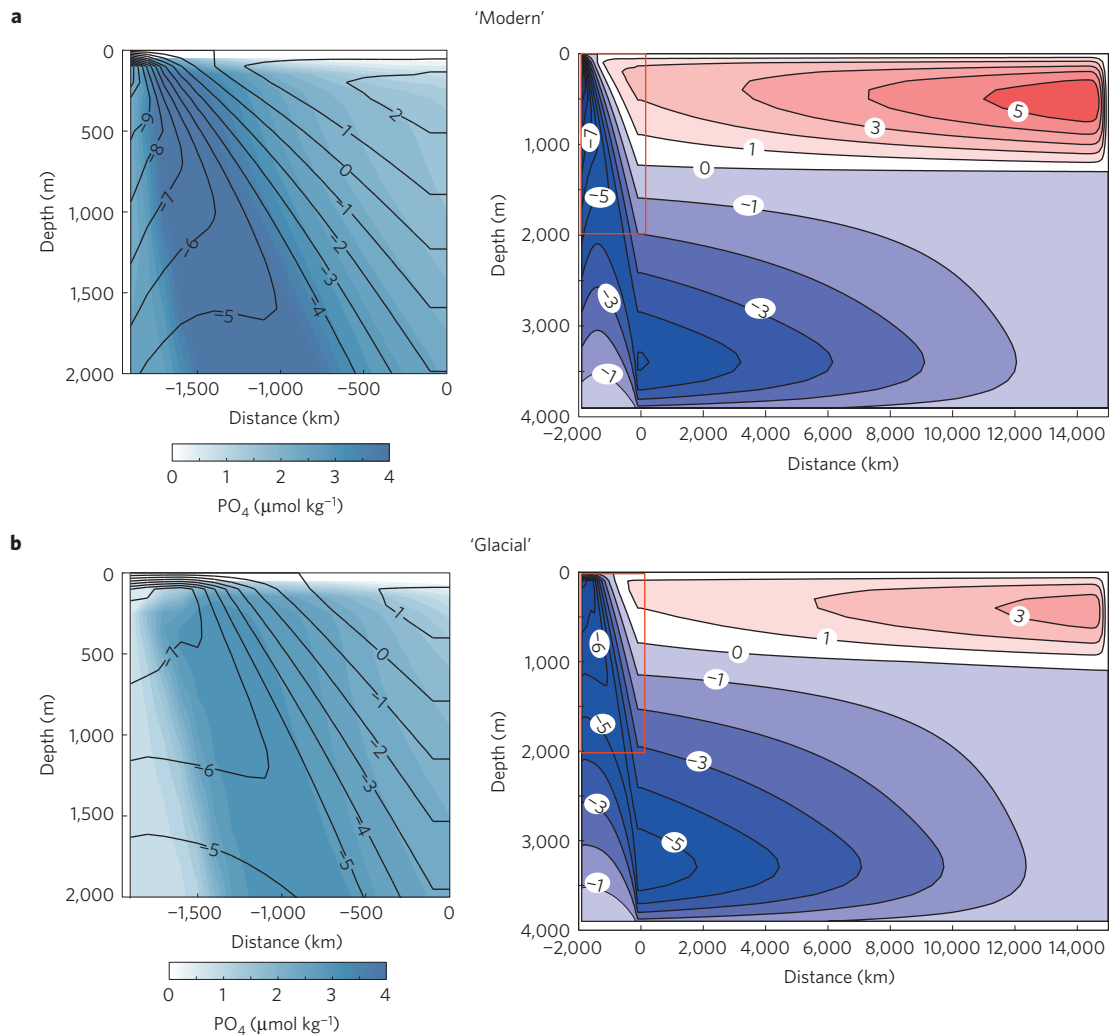


Figure 3 | Stream function and phosphate concentrations for ‘modern’ and ‘glacial’ forcings, from the model. Right-hand panels show stream functions (units of $10^6 \text{ m}^3 \text{ s}^{-1}$). The boundary between the southern channel and the northern basin is at the zero on the x axis. Red colours: clockwise circulation; blue colours: anticlockwise circulation; red rectangles mark the regions shown in detail in the left panels. Left panels: phosphate concentration (shading) and contours of stream function. **a**, ‘Modern’: high surface phosphate concentrations extend close to the southern boundary where the water sinks convectively. **b**, ‘Glacial’ simulation, less intense upwelling at greater distance from the southern boundary, results in preformed phosphate concentrations being lower in the sinking water.

Q.8

Q.9

Q.10

The strong upper interhemispheric cell present with modern forcing slows and shrinks as the southern buoyancy input is decreased, in agreement with most proxies that indicate a less extensive North Atlantic overturning at LGM (ref. 21). The two cells, which have linked circulations in the modern case, become more separate and distinct in their density range in the glacial simulation—an effect related to the separation of cells postulated for the glacial circulation¹³. The zone of higher net biological productivity supported by upwelling in the Antarctic moves northward, also consistent with proxies that indicate lower polar, but similar or higher subantarctic productivity^{23,24}. The glacial CO₂ reduction shown in Fig. 2b is that due to circulation changes alone—the direct effect of reducing the surface temperature is not included, and neither are ‘carbonate compensation’ effects. CO₂ reduction in the range 30–60 ppm is readily obtained for realistic forcing changes. The magnitude of the effect is dependent on other parameters, such as the wind stress profile, the northern buoyancy forcing and time constant chosen for biological drawdown. However, any change in the surface boundary conditions that leads to a northward shift of the southern upwelling region or reduced net upwelling, and hence a longer residence time for the upwelled, southward-moving surface waters before sinking

into the abyss, leads to a decrease in preformed nutrients and a reduction of atmospheric CO₂. Our results indicate that the effect occurs particularly robustly with an increased region of buoyancy loss in the south because the latitude of the upwelling region is then pushed northwards in order that the buoyancy budget is balanced.

The effect of iron fertilization, which has long been implicated in the lower LGM atmospheric CO₂ (refs 25–27), can also be incorporated into our simple model. Iron stimulates rapid growth of phytoplankton in southern polar waters²⁶, and its effect can be crudely emulated by making the biological response time τ_{bio} shorter in response to increased delivery of Fe. For the runs shown in Figs 2 and 3, halving τ_{bio} from 1 year to 6 months consistently further decreases CO₂, by 20–50 ppm. Increased and northward-shifted westerly winds have also been suggested as contributing to decreased atmospheric CO₂ in glacial time⁷, and the most important effect of such changes might also have been via the associated increases in buoyancy flux.

Our treatment shows that the hitherto-neglected mechanism of changed buoyancy forcing across the Southern Ocean can make a major contribution to lower glacial atmospheric CO₂. Our model solves self-consistently the dynamical equations for the

MOC, in an idealized geometry and in two dimensions. Thus, our calculations show the potential of buoyancy forcing to have a major influence on atmospheric CO₂, and capture the basic physical and biological mechanisms we expect to be important. We do not however distinguish between density change due to salinity and temperature variation, and in our model, deep water formation at the southern boundary is accomplished by full-depth convection (in common with most three-dimensional models), neglecting ice-shelf interactions that are important in bottom water formation in the real Southern Ocean.

Methods

Methods and any associated references are available in the [online version of the paper](#).

Received 15 April 2015; accepted 17 August 2015;
published online XX Month XXXX

References

- Siegenthaler, U. *et al.* Atmospheric science: Stable carbon cycle-climate relationship during the late pleistocene. *Science* **310**, 1313–1317 (2005).
- Shakun, J. D. *et al.* Global warming preceded by increasing carbon dioxide concentrations during the last deglaciation. *Nature* **484**, 49–54 (2012).
- Sigman, D. M., Hain, M. P. & Haug, G. H. The polar ocean and glacial cycles in atmospheric CO₂ concentration. *Nature* **466**, 47–55 (2010).
- Nikurashin, M. & Vallis, G. A theory of deep stratification and overturning circulation in the ocean. *J. Phys. Oceanogr.* **41**, 485–502 (2011).
- Nikurashin, M. & Vallis, G. A theory of the interhemispheric meridional overturning circulation and associated stratification. *J. Phys. Oceanogr.* **42**, 1652–1667 (2012).
- Marshall, J. & Speer, K. Closure of the meridional overturning circulation through Southern Ocean upwelling. *Nature Geosci.* **5**, 171–180 (2012).
- Toggweiler, J. R., Russell, J. L. & Carson, S. R. Midlatitude westerlies, atmospheric CO₂, and climate change during the ice ages. *Paleoceanography* **21**, PA2005 (2006).
- Tschumi, T., Joos, F. & Parekh, P. How important are Southern Hemisphere wind changes for low glacial carbon dioxide? A model study. *Paleoceanography* **23**, PA4208 (2008).
- Völker, C. & Köhler, P. Responses of ocean circulation and carbon cycle to changes in the position of the Southern Hemisphere westerlies at Last Glacial Maximum. *Paleoceanography* **28**, 726–739 (2013).
- Bouttes, N., Paillard, D. & Roche, D. M. Impact of brine-induced stratification on the glacial carbon cycle. *Clim. Past* **6**, 575–589 (2010).
- Stephens, B. B. & Keeling, R. F. The influence of Antarctic sea ice on glacial–interglacial CO₂ variations. *Nature* **404**, 171–174 (2000).
- Watson, A. J. & Naveira Garabato, A. C. The role of Southern Ocean mixing and upwelling in glacial–interglacial atmospheric CO₂ change. *Tellus B* **58**, 73–87 (2006).
- Ferrari, R. *et al.* Antarctic sea ice control on ocean circulation in present and glacial climates. *Proc. Natl Acad. Sci. USA* **111**, 8753–8758 (2014).
- Ito, T. & Follows, M. J. Preformed phosphate, soft tissue pump and atmospheric CO₂. *J. Mar. Res.* **63**, 813–839 (2005).
- Adkins, J. F., McIntyre, K. & Schrag, D. P. The salinity, temperature, and δ¹⁸O of the glacial deep ocean. *Science* **298**, 1769–1773 (2002).
- Karsten, R. H. & Marshall, J. Constructing the residual circulation of the ACC from observations. *J. Phys. Oceanogr.* **32**, 3315–3327 (2002).
- Talley, L. D. Closure of the global overturning circulation through the Indian, Pacific and Southern Oceans: Schematics and transports. *Oceanography* **26**, 80–97 (2013).
- Ledwell, J. R., Watson, A. J. & Law, C. S. Evidence for slow mixing across the pycnocline from an open-ocean tracer-release experiment. *Nature* **364**, 701–703 (1993).
- Toggweiler, J. R. & Samuels, B. On the ocean's large scale circulation in the limit of no vertical mixing. *J. Phys. Oceanogr.* **28**, 1832–1852 (1998).
- Samelson, R. M. Simple mechanistic models of middepth meridional overturning. *J. Phys. Oceanogr.* **34**, 2096–2103 (2004).
- Curry, W. B. & Oppo, D. W. Glacial water mass geometry and the distribution of δ¹³C of ΣCO₂ in the Western Atlantic Ocean. *Paleoceanography* **20**, PA1017 (2005).
- Arrigo, K. R. Sea ice ecosystems. *Annu. Rev. Mar. Sci.* **6**, 439–467 (2014).
- Jaccard, S. L. *et al.* Two modes of change in Southern Ocean productivity over the past million years. *Science* **339**, 1419–1423 (2013).
- Kohfeld, K. E., Le Quére, C., Harrison, S. P. & Anderson, R. F. Role of marine biology in glacial–interglacial CO₂ cycles. *Science* **308**, 74–78 (2005).
- Martin, J. H. Glacial–interglacial CO₂ change: The iron hypothesis. *Paleoceanography* **5**, 1–13 (1990).
- Watson, A. J., Bakker, D., Ridgwell, A., Boyd, P. & Law, C. Effect of iron supply on Southern Ocean CO₂ uptake and implications for glacial atmospheric CO₂. *Nature* **407**, 730–733 (2000).
- Martínez-García, A. *et al.* Iron fertilization of the subantarctic ocean during the last ice age. *Science* **343**, 1347–1350 (2014).

Acknowledgements

We thank J. R. Toggweiler and K. Speer for their constructive reviews. A.J.W. thanks the Royal Society for support under its Research Professorship scheme. G.K.V. acknowledges support from the Royal Society (Wolfson Foundation), a Marie Curie fellowship, and the NSF.

Author contributions

All authors contributed to the model development and concept. A.J.W. wrote the first draft and all authors contributed to revisions of the manuscript.

Additional information

Reprints and permissions information is available online at www.nature.com/reprints. Correspondence and requests for materials should be addressed to A.J.W.

Competing financial interests

The authors declare no competing financial interests.

1 Methods

2 **Overview of the model.** The ocean physical model is a numerical solution of the
3 global overturning circulation described in refs 4,5. This treats the zonally averaged
4 momentum and continuity equations in a two-dimensional (latitude and depth)
5 transformed Eulerian mean framework^{28,29} in a single, flat-bottomed,
6 interhemispheric basin that is closed except for a zonally periodic circumpolar
7 channel in the south, as seen in Fig. 3. To this is added a simple biogeochemical
8 scheme that solves for the distribution of nutrient and carbon in the ocean, and the
9 associated atmospheric CO₂ concentration. The model was run for 5,000 years to
10 achieve steady states of the circulation and carbon cycles, using an implicit
11 integration scheme and a time step of approximately 20 days. At each time step, the
12 dynamical scheme was first integrated in three regions as described below, followed
13 by integration of the biogeochemistry over the entire domain.

14 **Dynamical scheme.** The dynamical model (for which full discussion and
15 equations are given in refs 4,5) numerically time-steps the nonlinear
16 (advective–diffusive) buoyancy equation, with no-flux boundary conditions at the
17 bottom and side boundaries, and either a prescribed flux of buoyancy or a
18 relaxation to a prescribed buoyancy distribution at the surface, with the former
19 being used for the results shown in the paper. The buoyancy equation is solved
20 separately but consistently in three regions corresponding to the circumpolar
21 channel, the closed mid-latitude basin and a northern region of that basin in which
22 isopycnals outcrop, with a smooth matching of solutions between the three regions.
23 In the channel the (residual) velocity is obtained from a stream function that is the
24 sum of a wind-driven component and an eddy-induced flow, obtained from a
25 Gent–McWilliams style parameterization³⁰. In the closed basin region the
26 isopycnals are flat and the buoyancy equation reduces to a vertical
27 advection–diffusion equation. In the northern outcrop region convection is
28 assumed to produce isopycnals that extend vertically until they connect to the
29 horizontal isopycnals of the basin region, so potentially producing an isopycnal
30 pathway from the northern convective region to the circumpolar channel,
31 depending on the imposed buoyancy conditions at the surface.

32 **Boundary conditions and adjustable parameters.** The wind stress imposed at the
33 surface of the southern channel is shown in Fig. 2a, as are the buoyancy forcings for
34 different runs. The buoyancy forcing is imposed by specifying surface buoyancy
35 fluxes from the surface layer to the atmosphere in the southern channel. The
36 buoyancy over the northern basin does not enter the calculation, except in the
37 northern outcrop region, where it is relaxed towards a value given by

$$38 \quad B_n = 3 \times 10^{-3} + Y \times 1.5 \times 10^{-3} \text{ m s}^{-2}$$

39 where Y is the distance measured from the northern boundary in hundreds
40 of kilometres.

41 The vertical diffusivity increases with depth, from $2 \times 10^{-5} \text{ m}^2 \text{ s}^{-1}$ at the surface
42 to approximately $2 \times 10^{-4} \text{ m}^2 \text{ s}^{-1}$ at 4,000 m:

$$43 \quad K_v (\text{m}^2 \text{ s}^{-1}) = 2 \times 10^{-5} + 2 \times 10^{-4} \exp(-(4000 - z)/1000)/(1 - \exp(-4))$$

44 where z is depth measured in metres.

45 Sea ice is assumed to begin to form when the surface buoyancy declines below a
46 threshold value of $b_i = 10^{-3} \text{ m s}^{-2}$, where a buoyancy of zero is the densest water in
47 the model. The fraction of the surface covered by ice is given by $(1 - b/b_i)$ for
48 $b < b_i$. The effect of the ice is to block buoyancy flux and air–sea CO₂ flux; that is,
49 to reduce them by the fraction of sea ice coverage.

50 **Biogeochemical scheme.** Four tracers are carried in the model: phosphate (P),
51 dissolved inorganic carbon (DIC; C), total alkalinity (TA) and oxygen (O). The
52 tracers are transported using the same advection and diffusion scheme as
53 buoyancy, but with the addition of biogeochemical source and sink terms. At the
54 surface, P is relaxed towards zero with a time constant τ_{bio} set nominally at 1 year,
55 and O is relaxed to saturation with the atmosphere (taken as $343 \mu\text{mol kg}^{-1}$,
56 calculated at 2 °C and 35‰ salinity) with a time constant of one month. The
57 quantity of P removed by relaxation towards zero from the surface at each time step
is assumed to be fixed by the biota and instantaneously to sink into the underlying

58 water column, where it is returned to the dissolved form by respiration. The
59 maximum respiration rate at each depth is such that the particle flux decreases with
60 depth with a scale depth of 500 m. All material that reaches the bottom grid box is
61 remineralized there, so that the model conserves P overall.

62 Carbon and total alkalinity are removed from the surface and returned to the
63 water column with P, with constant Redfield ratios according to the following
64 scheme: $RC_{\text{org}}/P = 106$, $RC_{\text{inorg}}/C_{\text{org}} = 0.2$, $RN/P = 16$ (where C_{org} is soft-tissue
65 carbon, C_{inorg} is carbonate carbon, and N is nitrate). Nitrate appears in the scheme
66 because its removal and regeneration is accompanied by proton uptake or release,
67 so affects alkalinity.

68 These give the following stoichiometric ratios for removal/addition of DIC and
69 TA with P:

$$70 \quad \text{RDIC}/P = (1 + 0.2) \times 106 = 127.2$$

$$71 \quad \text{RTA}/P = 2 \times 0.2 \times 106 - 16 = 27.4$$

72 In addition, in subsurface waters, O is consumed by respiration in a ratio
73 $RO_2/P = -138$. The significance of keeping track of oxygen in this scheme is that
74 respiration must slow if oxygen becomes substantially depleted. We simulated this
75 by multiplying the maximum respiration rate by a factor O/100 if O drops below
76 100, where O is measured in micromoles per kilogram.

77 At the surface, the fugacity of CO₂ is calculated as a function of TA and C,
78 temperature and salinity, using the constants for the carbonate system in sea water
79 of ref. 31, refitted in ref. 32. The temperature and salinity used for these
80 calculations was fixed for all runs. As the focus of this study is the effects that
81 circulation change consequent on buoyancy forcing may have on atmospheric CO₂
82 concentrations, a clearer description is obtained if other variables affecting surface
83 CO₂ are constant. The salinity was fixed at 35‰ everywhere. The temperature was
84 a linear increase from 0 °C at the southern boundary to 12 °C at the northern edge
85 of the southern channel, a constant 12.4 °C over most of the northern basin, and a
86 linear decrease from 12.4 to 1.8 °C over the northernmost 1,500 km.

87 A single, well-mixed reservoir represents the atmosphere, and the air–sea
88 flux of CO₂ (calculated using the gas exchange equation with a fixed gas
89 transfer velocity) is subtracted or added to the surface, so that the total carbon
90 content of the ocean plus atmosphere is conserved. These carbon cycle
91 assumptions, namely conservation of nutrient and carbon and Redfield
92 stoichiometry, constitute the conditions under which surface preformed nutrient
93 is known to control atmospheric CO₂ (ref. 14). The model solves only for the
94 water masses involved in the overturning circulation and does not include the
95 warm and light waters of the subtropical gyres and the equatorial zone, which
96 are small in volume compared with the water masses sourced from the polar
97 oceans and therefore of secondary importance in setting atmospheric CO₂. A
98 similar but independently devised scheme has recently been applied to the
99 ocean's present-day carbon cycle (M. Nikurashin., T. Ito & G. Vallis, manuscript
100 in preparation).

101 **Code availability.** The MATLAB code used to generate the results in this paper is
102 available from the corresponding author.

103 References

- 104 28. Andrews, D. G. & McIntyre, M. E. Planetary waves in horizontal and vertical
105 shear: The generalized Eliassen–Palm relation and the mean zonal acceleration.
106 *J. Atmos. Sci.* **33**, 2031–2048 (1976).
- 107 29. Vallis, G. K. *Atmospheric and Oceanic Fluid Dynamics* 745 (Cambridge Univ.
108 Press, 2006).
- 109 30. Ferrari, R., Griffies, S. M., Nurser, A. J. G. & Vallis, G. K. A boundary-value
110 problem for the parameterized mesoscale eddy transport. *Ocean Model.* **32**,
111 143–156 (2010).
- 112 31. Mehrbach, C., Culbertson, C. H., Hawley, J. E. & Pytkowicz, R. M. Measurement
113 of the apparent dissociation constants of carbonic acid in seawater at
114 atmospheric pressure. *Limnol. Oceanogr.* **18**, 897–907 (1973).
- 115 32. Dickson, A. G. & Millero, F. J. A comparison of the equilibrium constants for
116 the dissociation of carbonic acid in seawater media. *Deep-Sea Res. A* **34**,
117 1733–1743 (1987).

Queries for NPG paper ngeo2538

Page 1

Query 1:

According to style, 'via' should be changed to 'through' or 'by means of' wherever possible. Can all three instances (which can be located using the search function in Adobe Reader) be changed to 'through'?

Query 2:

'which cause' changed to 'that cause' (rather than ', which cause') here, and similar changes made throughout the text. According to style, 'that' and 'which' are not interchangeable. 'That' should be used as a defining pronoun, whereas ', which' (note comma) should be used to introduce a further description. Please check that all text now follows this style, and that the intended meaning has been retained throughout. (All instances of 'that' and 'which' can be located using the search function in Adobe Reader.)

Query 3:

Please provide postcode for affiliation 4.

Query 4:

Please check the use of 'nutrient' versus 'nutrients' throughout. Are these all correct and as intended?

Query 5:

'While' changed to 'Whereas' here, to avoid non-time-related use of the former. OK?

Page 2

Query 6:

Text amended to 'a broader region of buoyancy loss' in the caption of figure 1b. OK?

Query 7:

Please check/amend the sentence 'Figure 2 shows Methods)' for clarity.

Page 3

Query 8:

Please check/amend the caption of figure 3b for clarity. Should, for example, the comma after 'simulation' be a colon, and should the comma before 'results' be removed?

Query 9:

Please note that reference numbers are formatted according to style in the text, so that any reference numbers following a symbol or acronym are given as 'ref. XX' on the line, whereas all other reference numbers are given as superscripts.

Query 10:

Please check the text here. Should it be, for example, 'and the time constant'?

Page 4

Query 11:

Acknowledgement to anonymous referee removed according to style.

Page 5

Query 12:

'while' changed to 'and' here, according to the query above. Please check, and amend if necessary.

Query 13:

Can 'of TA and C' be changed to 'of TA, C' here? And, in the next

sentence should 'The temperature and salinity ... was fixed' be 'The temperature and salinity ... were fixed'?

Query 14:

Any update for 'M.N., T.I. & G.V., manuscript in preparation'? (Note, only articles that have been published or are in the press can be included in the reference list; others can be listed as 'manuscript in preparation' in the text.)

Query 15:

Does the page number provided in ref. 29 represent the total number of pages in the book or the first page of the relevant page range? If the latter, please provide the final page number of that range.